CHEMISTRY
A EUROPEAN JOURNAL

ChemPubSoc
Europe

DOI: 10.1002/chem.201203890

VIP

Binary Compounds of Boron and Beryllium: A Rich Structural Arena with Space for Predictions

Andreas Hermann,*[a] N. W. Ashcroft,[b] and Roald Hoffmann[a]

Abstract: We explore ground-state structures and stoichiometries of the Be–B system in the static limit, with Be atom concentrations of 20% or greater, and from $P=1$ atm up to 320 GPa. At $P=1$ atm, predictions are offered for several known compounds, the structures of which have not yet been determined experimentally. Specifically, at 1 atm, we predict a structure of $R\bar{3}m$ symmetry for the compound Be_2B_3, seen experimentally at high temperatures, which contains interesting BeBBBBe rods; and for the compound BeB_4 we calculate metastability with respect to the elements with a structure similar to MgB_4, which is quickly replaced as the pressure is elevated by a *Cmcm* structure that features 6- and 4-membered rings in B cages, with Be interstitials. For another high-temperature compound, Be_2B, we confirm the CaF_2 structure, but find a competitive and actually slightly more stable ground-state structure of $C2/m$ symmetry that features B_2 pairs. In the case of BeB_2, a material for which the stoichiometry has been the subject of debate, we have a clear prediction of a stable $F\bar{4}3m$ structure at $P=1$ atm. It has a diamondoid structure that is based on cubic (lower P) or hexagonal (higher P) diamond networks of B, but with Be in the interstices. This Zintl structure is a semiconductor at low and intermediate pressures. At higher pressures, BeB_2 dominates the phase diagram. In general, the Zintl–Klemm concept of effective electron transfer from the more electropositive ion and bond formation among the resulting anions has proven useful in analyzing the structural preferences of many compositions in the Be–B system at $P=1$ atm and at elevated pressures. An unusual feature of this binary system is that the 1:1 BeB stoichiometry never appears to reach stability in the static limit, although it comes close, as does $Be_{17}B_{12}$. Also stable at high pressures are stoichiometries BeB_3, BeB_4, and Be_5B_2.

Keywords: beryllium · boron · density functional calculations · high-pressure chemistry · phase transitions

Introduction

Beryllium and boron, neighbors in the periodic table with element numbers four and five, could hardly be more different in their elemental properties. Under standard conditions, beryllium crystallizes in a hexagonal close-packed (hcp) structure, and when compressed does not undergo a phase transition up to pressures of 200 GPa[1] (it is predicted to transform into a body-centered cubic (bcc) phase around 400 GPa).[2] Boron, on the other hand, crystallizes in a variety of complex structures that feature icosahedra as a familiar motif. This is, of course, related to the electron deficiency of the boron, which drives its tendency to form multicenter bonds.[3] Elemental boron readily transforms into yet other structures under moderate pressure and at low to moderate temperatures.[4–11]

Although beryllium is a metal, in a sense it is barely so. Its density of states (DOS) at the Fermi level is low; the Fermi level reveals itself in a deep pseudogap that separates 2s from 2p states. In a way, $Be(1s)^2(2s)^2$ is akin to $He(1s)^2$, and, indeed, its chemistry is meager. Be is a superconductor, albeit with a surprisingly low transition temperature T_c (considering that its Debye temperature is exceedingly high).[12] Boron is a semiconductor but becomes a metal and also a superconductor at very high pressures.[13] Both elements have their applications: beryllium as window material in X-ray equipment, as a wall liner in plasma fusion reactors,[14] or as a stiff lightweight material in aerospace applications; boron as a neutron moderator in nuclear reactors, or as a superhard material by itself or as a key ingredient in alloys.[15]

What might happen if these two elements were brought together? The known beryllium–boron phase diagram (Figure 1, which includes the liquid region) features a variety of boron-rich phases, several high-temperature phases, and the Be_4B phase as the only beryllium-rich phase that is stable at room temperature.[16,17] In a previous study, we have studied the $P=1$ atm properties of compounds BeB_n with $n=2$–4.[18] No crystallographic information is available for the high-temperature Be_2B_3 compounds or for the BeB_4 compound, and no high-pressure information appears to be available for any of the phases, at least in the unclassified

[a] Dr. A. Hermann, Prof. Dr. R. Hoffmann
Department of Chemistry and Chemical Biology
Cornell University, Ithaca, NY 14853 (USA)

[b] Prof. Dr. N. W. Ashcroft
Laboratory of Atomic and Solid State Physics
Cornell University, Ithaca, NY 14853 (USA)

Supporting information for this article is available on the WWW under http://dx.doi.org/10.1002/chem.201203890.

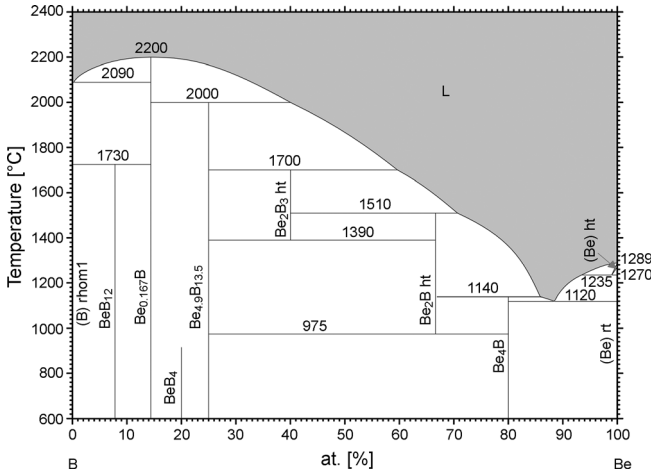

Figure 1. The experimental beryllium–boron binary phase diagram at $P=$ 1 atm. We will focus on the low-temperature region. Reprinted with permission of ASM International. All rights reserved. http://www.asminternational.org.

literature. The compounds with higher boron content are generally not well characterized but probably contain B_{12} icosahedra with beryllium occupying interstitial sites.[19] It could well be that the known health risks of working with beryllium and its oxide have (appropriately) limited the exploration of the compounds of the element.

Some of the known phases in the Be–B phase diagram are metallic. These include as noted pure beryllium, the Be-rich Be_4B phase, and the $Be_{4.9}B_{13.5}$ phase (or "$BeB_{2.75}$"); see below. For other phases, the electronic properties are not known; it should be expected that compounds with higher beryllium content are more likely to assume a metallic state, and we will comment on the specific cases in the discussion below.

Here, we engage high-level numerical and computational methods to study beryllium–boron compounds in their static ground-state conditions by using density functional theory (for details, see the Supporting Information and references therein).[19–33] Finite temperature effects are not included in our calculations, but we assess the dynamic stability of the various candidate compounds. Even though beryllium and boron are relatively light elements, ground-state enthalpy differences between different phases are usually large enough that we do not expect them to be affected qualitatively by the omission of dynamic contributions. For a representative set of structures of BeB_2, including a variety of binding scenarios, zero-point energies at $P=1$ atm are within 10–20 meV per atom of each other. We concentrate on the beryllium-rich side of the phase diagram and avoid the complex boron-rich compounds (BeB_m with $m>4$), which often appear with partial occupancies and very large unit cells. For various stoichiometries, we examined structure types found in other combinations of Group 2–13 elements in the Inorganic Crystal Structure Data (ICSD) database.[34,35] And for selected stoichiometries and pressures we performed unbiased structure searches by using evolutionary algorithms[25,36–39] to obtain low-enthalpy structural candidates.

Results and Discussion

Molecular beryllium–boron compounds: If their structures are available, molecular compounds provide us with a $P=$ 1 atm guidepost for a reasonable B–Be bonding interaction. Beryllium chemistry is not extensive;[40] there appears to be only one compound that has a direct, unsupported Be–B bond, the X-ray diffraction structure of which has been determined, as shown in Figure 2a, with a B–Be separation of 2.05 Å.[41]

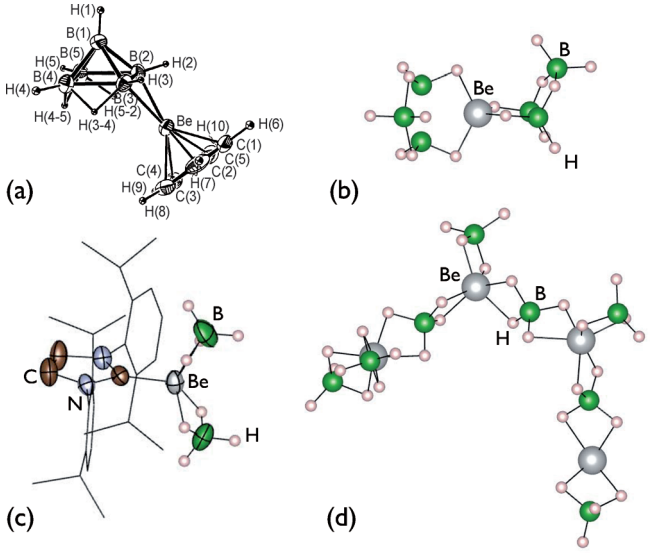

Figure 2. A selection of molecular compounds containing linked Be–B units: a) $(B_5H_8)BeCp$, b) $Be(B_3H_8)_2$, c) $(C_3N_2R_2)Be(BH_4)_2$, and d) polymeric $Be(BH_4)_2$. Large gray (medium green, small white) spheres indicate beryllium (boron, hydrogen) atoms; other atoms are labeled. Figure part (a) reprinted with permission from ref. [41]; copyright 1979 American Chemical Society.

A number of beryllium borohydrides in which the B and Be atoms are linked by hydrogen bridges, and in which the separation of the two heavier atoms is quite short, also exist. The parent structure of these is an old compound, $Be(BH_4)_2$, synthesized by Burg and Schlesinger in 1940[42] (for a history of this compound, see also ref. [43]). The crystal structure of $Be(BH_4)_2$, in the polymeric form shown in Figure 2d, was determined by Marynick and Lipscomb.[44] It contains a helical polymer with two hydrogen bridges between Be and B, and the bridged Be–B separations are 1.97 and 2.00 Å. A similar bonding type is found in $Be(B_3H_8)_2$, with Be–B distances of 1.97–1.98 Å.[45] Recently, a carbene-stabilized complex of $Be(BH_4)_2$ was synthesized, with Be–B separations of 1.95 and 1.96 Å.[46]

The bonding in the latter group of compounds is expected to be mainly through the hydrogen bridges, although, just as in the archetypical diborane (B_2H_6), there remains a core

ambiguity about the extent of Be–B direct bonding in these bridged structures. In any event, just from these few examples it is clear that Be–B separations of 1.95–2.05 Å are normal in molecules. And similar distances have been found in the crystal structure of BeB_2C_2, with Be–B separations of 2.02–2.07 Å.[47]

Experimentally known solid phases, enthalpies, and properties: In Figure 3, we plot the relative enthalpies of formation ΔH_f in the ground state with respect to the crystalline solid phases of elements Be and B, as obtained from our calculations, over a range of pressures and for four stoichiometries: the experimentally well-characterized Be_4B and Be_2B, and two compounds whose crystal structure are unknown, Be_2B_3 and BeB_4, but for which we have made the best structural estimates available to us (see below for details). We will discuss other stoichiometries as well.

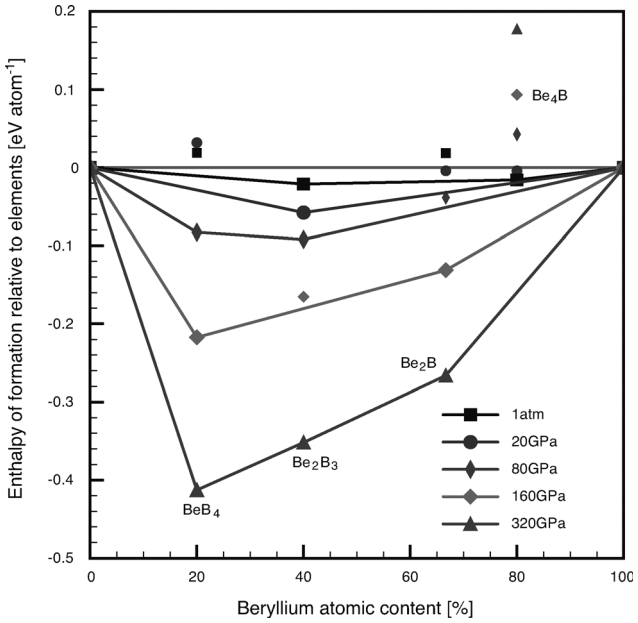

Figure 3. Relative ground-state enthalpies of formation per atom for the experimentally known Be_xB_y stoichiometries, depending on Be atomic content, and for various pressures. This is not the complete theoretical phase diagram, as it does not yet include some new stoichiometries we predict here.

A negative enthalpy of formation indicates that the mixture is more stable than the separated elements. The convex hull of all known ΔH_f values at a given pressure gives the stable mixtures in the ground state, with respect to decomposition into other binary or unary phases. At $P=1$ atm, we find only Be_4B and Be_2B_3 to be stable (next to the elemental crystals of beryllium and boron). The high-temperature phase Be_2B in our calculations is unstable in the ground state with respect to B and Be_4B by less than 100 meV per atom. Under pressure, Be_2B becomes much more stable, as we will see, whereas Be_4B shows the opposite behavior. Thus, at a pressure of $P=80$ GPa, the reaction $Be_4B(s) \rightarrow 2\,Be(s) + Be_2B(s)$ would have a negative ΔH_f ("(s)" indicates that we compare the solid phases here), whereas at $P=1$ atm it would have a positive ΔH_f. However, other "escape routes" are possible, and more (ideally, all) stoichiometries of Be_xB_y have to be studied to ascertain the stable phases.

Below, we discuss briefly the experimentally known structures, followed by a discussion of proposed structures for other experimentally known stoichiometries. We caution the reader that our especial composition trajectory, chosen for clarity in a complex phase diagram, means that Figure 3 is not yet the complete theoretically predicted phase diagram. Other, new stoichiometries might well enter the picture, and some of the phases shown in Figure 3 might turn out not to lie on the convex hull. The complete calculated phase diagram will be shown below.

Be_4B: This structure crystallizes in space group 129, *P4/nmm*, with two formula units per unit cell. As seen in Figure 4, Be_4B can be viewed as an ABC stacking, in which "A" and "C" are slabs of a base-centered tetragonal Be lattice with a boron atom each on one of the faces, and "B" is a fully face-centered tetragonal Be lattice slab.[48]

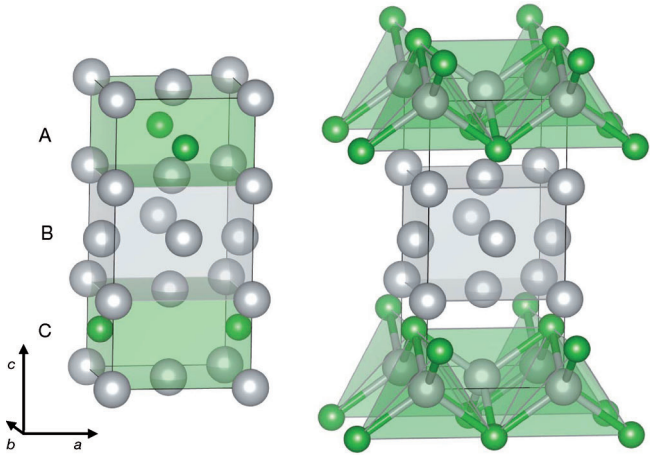

Figure 4. Left: Experimental (room-temperature) Be_4B crystal structure. Right: Optimized theoretical Be_4B crystal structure (ground state) at $P=1$ atm, with a different definition of the sublattices (shaded); see text. Gray (green) spheres denote beryllium (boron) atoms.

Alternatively, and this is visualized in the right-hand panel of Figure 4, the structure can be seen as composed of alternating layers of a face-centered tetragonal Be lattice with those of a BeB lattice of Be-centered boron tetrahedra that share vertices and faces. This view helps us understand why the boron atoms in the "A" and "C" base-centered tetragonal Be lattices are not in the center of the respective Be face: this would result in strained boron tetrahedra. Another variant would be to place the boron atoms in the "A" and "C" layers on the same Be faces, thus replacing the boron tetrahedra with planar arrangements. This costs about 1.2 eV per unit cell; the formation of Be-centered tetrahedra is then clearly favored here.

Table 1. Structural parameters of the P_4/nmm phase of Be_4B, from calculations and experimental (room-temperature) data. The atomic positions are given in fractional coordinates.

	a [Å]	c [Å]	V [Å^3]	Be_1	Be_2	B
Exptl[48]	3.38(1)	7.06(2)	80.7(7)	0 0 0.304	0 0.5 0.481	0 0.5 0.169
this work, ground state	3.35	7.00	78.6	0 0 0.305	0 0.5 0.481	0 0.5 0.169

The structural parameters of the optimized ground-state structure agree very well with experimental room-temperature data, as shown in Table 1. The Be–Be separations in the "B" layer are as short as 2.08 Å (slightly shorter than in pure beryllium with d(Be–Be) = 2.21 Å); and the B–Be separations are between 2.08 and 2.37 Å (longer than B–Be separations in molecules with hydrogen bridges between Be and B: 1.78[49] or 1.92 Å;[44] but comparable with separations in molecules with direct Be–B bonds of 2.05 Å).[41]

Be_4B is a metal, but as with Be it features a pronounced pseudogap in its density of states (DOS) around the Fermi energy (see Figure 5). Interestingly, the DOS is basically

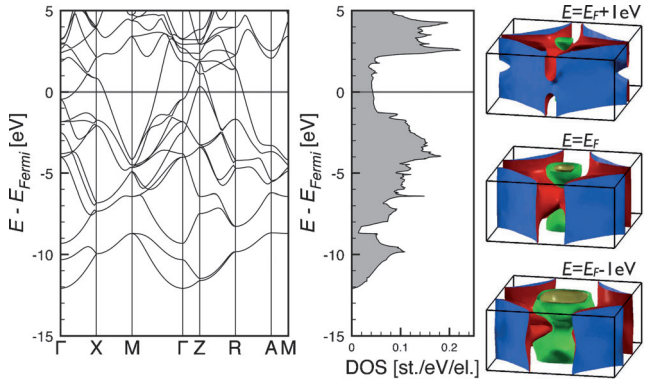

Figure 5. From left: Electronic band structure, density of states per electron, and Fermi surface of Be_4B, at $P = 1$ atm. Also shown are constant energy surfaces above and below the Fermi energy.

constant around the Fermi energy. Note from the band structure that along several directions in the Brillouin zone steep bands cross the Fermi level; their approximate linearity around the Fermi level can be related to the flat DOS near that energy. The states in this energy region are mostly localized around the beryllium atoms in layer "B".

An evolutionary structure search at $P = 60$ GPa with $Z = 2$ formula units per cell did not reveal any other competitive structure; hence we believe the $P4/nmm$ structure to be the optimal one for this stoichiometry, even at elevated pressures and possibly temperatures. However, as Figure 3 shows, Be_4B does not survive an increase in pressure; it becomes unstable with respect to elementary Be and other binaries of beryllium and boron.

Be_2B: The high-temperature Be_2B phase crystallizes in the cubic fluorite CaF_2 structure, space group 225, $Fm\bar{3}m$, with four formula units per conventional unit cell.[33] Two other X_2Y structures are found among the Group 2/Group 13 binaries: one is the Mg_2In structure (space group 189, $P\bar{6}2m$, three formula units per cell),[50] the other is the closely related Mg_2Ga structure (space group 190, $P\bar{6}2c$, with six formula units per cell).[51] These three structures are shown in Figures 6 and 8 (structural information for these and all other phases discussed here can be found in the Supporting Information). The Mg_2Ga structure is also found in a system with a very different electron count, namely, Li_2Sb.[52,53]

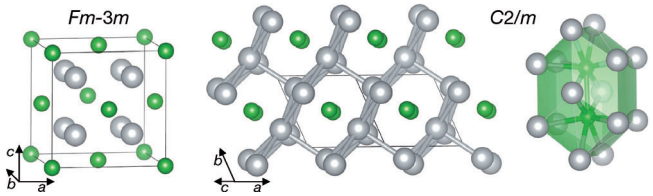

Figure 6. Left: Be_2B in the ground-state CaF_2 structure. Middle: the $C2/m$ structure, at $P = 1$ atm. Right: Coordination polyhedron of B_2 units in the $C2/m$ structure.

Of these three ground-state structures, the CaF_2 structure is the most stable at atmospheric pressures, but it becomes unstable with respect to both hexagonal structures as pressure increases (see Figure 7). Our optimized CaF_2 lattice constant of 4.57 Å agrees well with the experimental value of 4.663 Å.[33] We also performed evolutionary structure searches for Be_2B, at $P = 1$ atm with four formula units in the unit cell, and at $P = 160$ GPa with six formula units in the unit cell. The resultant low-enthalpy structure at atmospheric pressure has $C2/m$ symmetry and two formula units in the unit cell. The $C2/m$ structure is also shown in Figure 6. It consists of a (significantly distorted) network of hexagonal Be channels, and B dimers within those channels

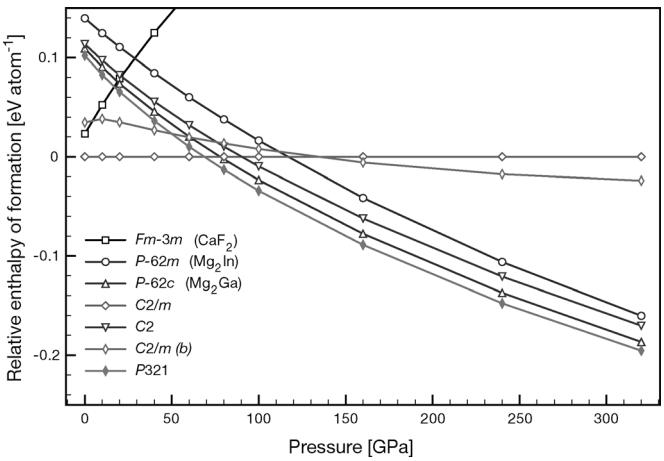

Figure 7. Ground-state enthalpies per atom of various Be_2B crystal structures, relative to our predicted low-enthalpy $C2/m$ structure. The structure labeled $Fm\bar{3}m$ is the CaF_2 structure.

(they run into the plane of the paper in Figure 6). Each B_2 unit is surrounded by a Be_{14} polyhedron. The B–B separation of 1.94 Å is significantly longer than in solid boron at $P=1$ atm (for which d(B–B) = 1.66 Å for 2c–2e interactions, and 1.75–1.80 Å for icosahedral multicenter bonds), but it is within the range of a bonding interaction.

In an ionic picture, where each beryllium atom adopts Be^{2+}, each boron atom is also formally B^{4-}, one short of an octet. It makes sense that such 7-electron B atoms would then dimerize to form formal B_2 units (the charge will be screened by Be^{2+} ions) that are isoelectronic to F_2.

We see here once again the workings of the Zintl–Klemm formalism.[54–56] In this most useful solid-state chemistry concept, in an A_xE_y compound in which A is an electropositive element (alkali metal or alkaline earth) and E a more electronegative main-group element, one first anticipates electron transfer from A to E, followed by octet-dictated bond formation among the larger A anions.

Interestingly, we find that at $P=1$ atm the static $C2/m$ structure has a lower total energy than the experimentally observed CaF_2 structure (by just 70 meV per formula unit). Accordingly, we would therefore encourage an experimental search for this structure.

As the pressure is raised, new ground-state structures evolve for Be_2B (see Figure 7). These are based on the Mg_2In $P\bar{6}2m$ structure shown in Figure 8. A little lower in enthalpy is also a $P\bar{6}2c$ structure (found in Mg_2Ga), in which two out of the three B chains in the unit cell undergo what could be viewed as a Peierls distortion, a pairing to form B_2 units (the B–B separation is 1.71 Å in a pair at 100 GPa). And lower still in enthalpy, but by just 30 meV per formula unit at 100 GPa, is a $P321$ structure, the most stable we have found. In the Supporting Information we discuss the transformations between these structures in greater detail. Similar structural motifs of boron chains in atomic channels are seen in the slightly boron-deficient system LiB_{1-x} ($x=0$–0.2), in which Li atoms form a hexagonal sublattice, the channels of which along the [0001] direction are filled by equidistant chains of boron atoms, which are non-commensurate with the Li sublattice.[29,57,58]

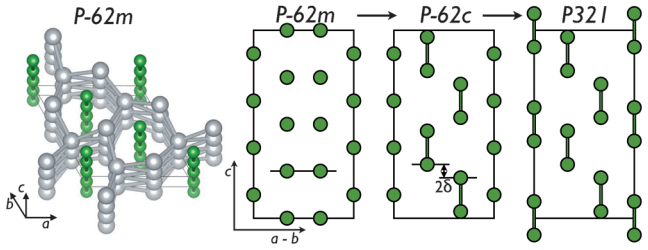

Figure 8. Left: The ground-state $P\bar{6}2m$ structure of Be_2B at $P=160$ GPa; From middle to right: Cuts through the [1120] plane of the respective unit cells of $P\bar{6}2m$, $P\bar{6}2c$, and $P321$ (not to scale), with B atoms shown as green spheres. Atomic displacement (δ) is indicative of B–B dimerization.

The structures we find are metallic, as could probably be expected because of the high beryllium content. Whereas the CaF_2 structure observed at $P=1$ atm is actually a very good metal, as judged by its density of states near the Fermi energy, the other structures feature quite deep pseudogaps around the Fermi energy (Figure 9); these structures are rapidly stabilized by pressure. The CaF_2 structure for Be_2B has been proposed as a potential superconductor,[59] and its transition temperature has been estimated as $T_c=5$–10 K.[60] But the computed enthalpies suggest that this phase has little chance of surviving compression.

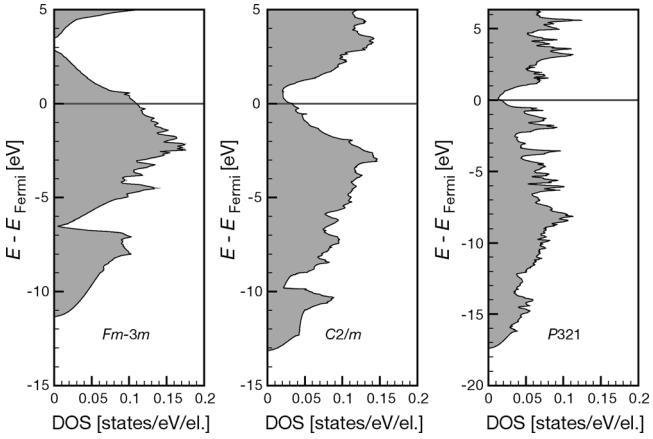

Figure 9. Electronic densities of states per electron of various Be_2B phases: $Fm\bar{3}m$ and $C2/m$ at $P=1$ atm; and $P321$ at $P=160$ GPa. All are clearly metallic.

Be_2B_3: A high-temperature compound ($T>1390$ °C) of Be_2B_3 stoichiometry has been reported, but no details of its crystal structure are available thus far.[16] The only other X_2Y_3 compound in Groups 2/Group 13 that we are aware of is Mg_2Al_3, the atoms of which are known to randomly occupy the sites of a face-centered cubic (fcc) lattice.[61]

We performed an evolutionary structure search on Be_2B_3 binaries at $P=80$ GPa, with two formula units per cell. The relative enthalpies of the most promising candidate structures are compiled in Figure 10, and the most stable structure at $P=80$ GPa (and at all lower pressures) is of $R\bar{3}m$ symmetry (see Figure 11).

This structure features linear Be-B_3-Be units along the rhombohedral [111] directions, or hexagonal c axis, not unlike what is seen, for example, in the Bi_2Te_3 structure.[62] In the latter, however, the atoms are not actually bonded along the c axis, unlike the Be_2B_3 structure found here. At $P=1$ atm, the atomic separations along the Be-B_3-Be units are Be–B = 1.82 Å and B–B = 1.73 Å, both of which are definitely of bonding-contact character, as judged by structures of molecular compounds cited above. All boron atoms are eightfold coordinated (see Figure 11), whereas the "terminating" beryllium atoms are sevenfold coordinated, but with an empty coordination site along the c axis.

One can interpret this structure in a rather different way as well. We might see in it the special features of Be_2B

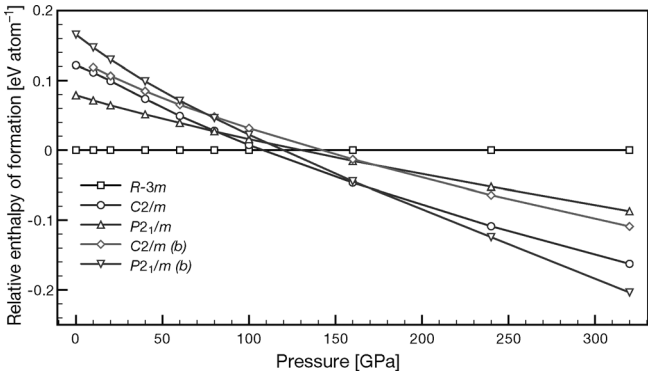

Figure 10. Relative enthalpies of possible ground-state structures for Be_2B_3, as dependent on pressure and scaled relative to the low-pressure $R\bar{3}m$ phase.

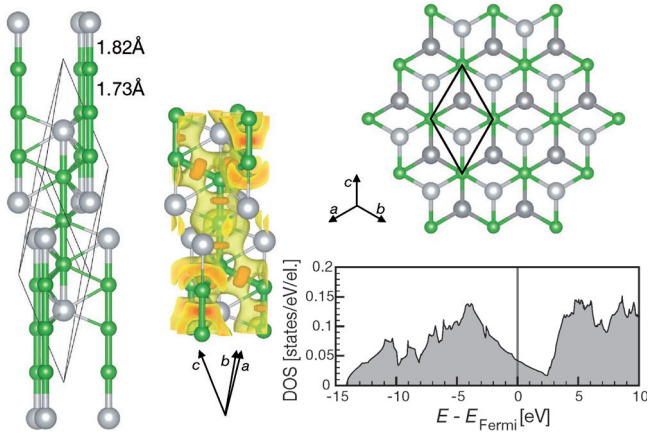

Figure 11. The $R\bar{3}m$ ground-state structure of Be_2B_3 at $P=1$ atm. Left: Rhombohedral unit cell, centered on the Be-B_3-Be unit (thick bonds drawn), and thin bonds drawn between these units (with $d=1.93$–2.06 Å). Middle: ELF isosurface plot, centered on the Be-B_3-Be unit. Orange (yellow) surfaces are drawn at ELF = 0.80 (0.65). Right: Top view onto the Be_2B layer in the hexagonal basal plane (two shades of Be atoms are for atoms above and below the plane), and electronic DOS per electron.

sheets in the hexagonal basal plane, which alternate with graphitic-like boron nets along the hexagonal c axis. In Figure 11, a top view of the Be_2B sheets is shown: the boron nets are buckled, with all beryllium atoms positioned above or below the plane of the boron atoms. The latter are then the central atoms of the ensuing linear Be-B_3-Be units.

An analysis of the electron localization function (ELF)[63] for the $R\bar{3}m$ structure shows bonding within and between the Be-B_3-Be units (see Figure 11). The highest ELF values, found between adjacent boron atoms (typically about 0.85), indicate covalent-like bonding between these, but ELF maxima are also found between beryllium and its neighboring boron atoms. It follows that, whereas the linear Be-B_3-Be unit is an essential feature of the $R\bar{3}m$ structure, Be_2B_3 is basically still a three-dimensional solid.

The electronic DOS also corroborates this (see Figure 11): features indicative of a low-dimensional electronic structure—for instance, BeB_3Be "molecules"—are missing. Instead, the DOS is dominated by an impressive pseudogap (Be_2B_3 is metallic in our calculations, thus revealing yet another metallic Be–B compound). To reach the bottom of this pseudogap, one would need a total valence electron count of 14 (the Be_2B_3 unit cell has 13 valence electrons). This suggests a BeB_4 stoichiometry, which we have studied and comment on below. Other ground-state structures (of $C2/m$ and $P2_1/m$ symmetry) become stable with respect to the $R\bar{3}m$ structure at pressures above 100 GPa (typical compression $V_0/V=1.4$). These are discussed in the Supporting Information; no Be_2Be_3 structure appears on the convex hull above 80 GPa.

If we follow the experimental $P=1$ atm phase diagram (Figure 1), crystals that correspond to the compositions we just discussed (Be_2B and Be_2B_3) should decompose into Be_4B and $Be_{4.9}Be_{13.5}$ (or "$BeB_{2.75}$"; see below), whereas we are now finding them to be stable compounds (see Figure 3). The discussion of the complicated "$BeBe_{2.75}$" phase below will shortly resolve this issue.

BeB_4: This stoichiometry is also known experimentally at room temperatures, even though no details of its crystal structure are available to date.[16] The same stoichiometry is, however, found in a variety of Group 2/Group 13 binaries: MgB_4, in *Pnam* symmetry, with four formula units per unit cell;[64] CaB_4, in *P4/mbm* symmetry, with four formula units per cell (small amounts of added carbon or external pressure seem necessary for its synthesis);[65–67] the $BaAl_4$ structure type of *I4/mmm* symmetry with two formula units per cell, which is also found in the $CaGa_4$, $SrGa_4$, $BaGa_4$, and $BaIn_4$ systems;[68] and a distorted variant of the last structure, with $C2/m$ symmetry and two formula units per cell, as found in $CaGa_4$.[69]

Clearly, there is room for a theoretical prediction of the structure of BeB_4 here, and elsewhere[18] we have discussed the properties of this compound at $P=1$ atm in great detail, together with other boron-rich Be–B compounds (see also below). Here we give only a short summary of the properties of BeB_4 at atmospheric pressure, and then concentrate on the high-pressure phase transitions.

At $P=1$ atm, we find that BeB_4 is most stable in a structure of $P2_12_12_1$ symmetry, which is closely related to the MgB_4 structure type. It is still, however, unstable with respect to stoichiometric decomposition into the crystal structures of the elements (see Figure 3 and ref. [18]). The $P2_12_12_1$ structure features a 3D boron network with beryllium atoms in interstitial sites (see Figure 12, inset). The main structural motifs of the boron sublattice are singly capped edge-sharing pentagons, with bonds that involve the "capping" B atoms then providing the three-dimensional structure. The B–B separations in this structure range from 1.63 to 1.82 Å; however, Be–B separations are 1.91 Å or longer (as discussed for the Be_4B compound above, and not unusual in molecular compounds with Be–B bonds), and the beryllium atoms are located close to the centers of the largest cavities within the unit cell.

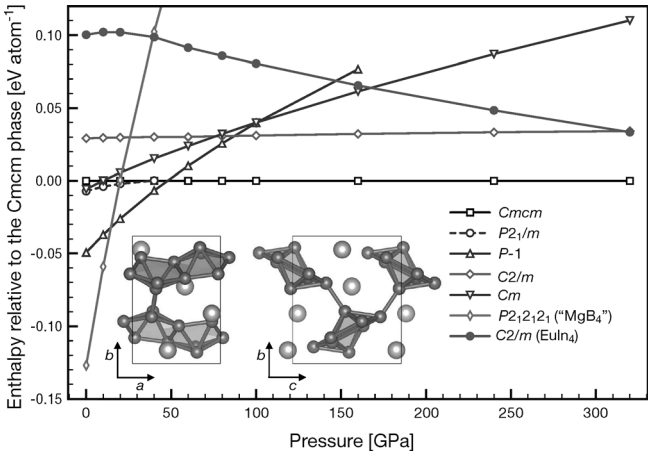

Figure 12. Ground-state enthalpies of formation of various BeB_4 crystal structures, relative to the high-pressure phase of *Cmcm* symmetry (see text). The last two structures correspond to (or are derived from) known structure types, see text. Inset shows two views of the $P2_12_12_1$ structure at $P=1$ atm.

A ground-state structure of $R\bar{3}m$ symmetry, constructed from the $R\bar{3}m$ structure of Be_2B_3 discussed above by replacing one beryllium atom with a boron atom, is not stable at atmospheric or indeed any higher pressures. However, under pressure, the $P2_12_12_1$ structure also becomes rapidly unstable with respect to a variety of other structures we have obtained from an evolutionary structure search (with two formula units per cell and at $P=80$ GPa). The first of these, of $P\bar{1}$ symmetry and dynamically stable, becomes stable with respect to the $P2_12_12_1$ structure around $P=$ 15 GPa. It features a boron network similar to the $P2_12_12_1$ structure, but with severely distorted capped pentagons, and with beryllium atoms again in rather asymmetrical interstitial positions.

At higher pressures we do find BeB_4 to be a stable stoichiometry in the Be–B system, indeed highly stable. A *Cmcm* structure we found in our structure search emerges as the most preferred enthalpically, and this structure is the global minimum for BeB_4 if pressures are $P=50$ GPa or higher (see Figure 12). It is also dynamically stable at $P\geq$ 40 GPa (at lower pressures it is a saddle point on the potential-energy surface, and the enthalpy of its formation can be lowered slightly through a distortion to a lower symmetry $P2_1/m$ structure; see Figure 12). In the Supporting Information we discuss the $CaGa_4$ alternative (in the original structure-type space group $C2/m$, but optimized in the space group $Fmm2$) with similar structural features, but always with higher ground-state enthalpy; the local environment of the Be atoms in the $CaGa_4$ structure type (a cage of two six-membered B rings in "boat" conformation) is also found at the metal atoms in MnB_4 and CrB_4.[70,71]

The high-pressure *Cmcm* structure (Figure 13) features a 3D boron network with beryllium atoms in interstitial positions, a geometry much more "regular" than in the structures stable at $P=1$ atm. There are "layers" of boron atoms in the *ab* plane, which are bonded along the *c* axis, and alternate with layers of interstitial beryllium. In particular, the boron layers in the *Cmcm* structure feature rows of edge-sharing buckled six-membered boron rings. The layers are in turn connected through four-membered boron rings. The beryllium atoms are then sandwiched between buckled B_6 rings, which are in a "chair" conformation (a wurtzitane-like environment, see the coordination polyhedra of Be indicated in Figure 13). The boron network immediately surrounding the Be atoms has the interesting structure of hexagonal diamond, lonsdaleite.

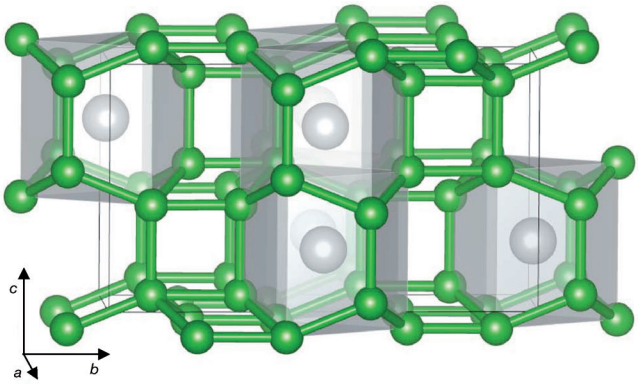

Figure 13. The ground-state *Cmcm* crystal structure of BeB_4 obtained from evolutionary structure search, at $P=80$ GPa. Be coordination polyhedra are indicated.

The *Cmcm* structure (more precisely, its boron sublattice) repeats structural features of *Z* carbon, a proposed new phase for compressed cold graphite.[72] However, if we use the *Z*-carbon structure itself to establish the boron sublattice and occupy its cavities selectively with beryllium atoms, we find it not to be a competitive structure for BeB_4 at any pressure.

Were the four-membered rings in the *Cmcm* structure reduced to single B–B bonds along *c* by removing two boron atoms per ring (thus creating buckled graphitic sheets in the *ab* plane), the stoichiometry would be BeB_2 and the structure-type $CaIn_2$, which we actually do find as a stable high-pressure phase for BeB_2; see the discussion below. There, the boron sublattice indeed has the hexagonal diamond lonsdaleite structure.

Filling the gaps—other stoichiometries: So far we have discussed only the simpler known stoichiometries. It is now time to introduce the more complete (and complex) Be–B phase diagram shown in Figure 14. It includes the very stable (at $P=1$ atm) "$BeB_{2.75}$" phase (experimental assignment $Be_{29.5}B_{81}$),[18] as well as BeB_2, BeB_3, BeB_4, and Be_5B_2. There are also phases that make up (or come close to) the convex hull at higher pressures, including the "missing" 1:1 stoichiometry.

Compounds with 20 to 33 % of atomic beryllium content: At $P=1$ atm, and around room temperature, this region of the phase diagram (it includes the compositions BeB_x with $x=$ 2–4) has been the subject of much experimental uncertainty

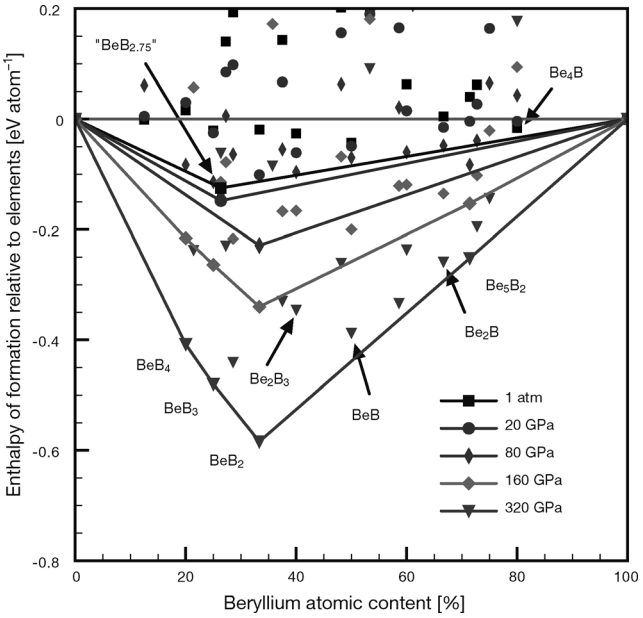

Figure 14. Relative ground-state enthalpies of formation per atom for all Be–B phases included in this study.

and debate over the years. We believe we might now have clarified the complex structural story, which features off-stoichiometry structures, vacancies, and partial occupations, in a separate publication,[18] so we will only summarize those $P=1$ atm results briefly for each compound and then move on to high-pressure effects by proceeding sequentially.

BeB_2: The stoichiometry BeB_2 has been the subject of extensive experimental studies that span several decades.[33,73–76] The most recent single-crystal X-ray diffraction studies assigned it the stoichiometry "$BeB_{2.75}$", which crystallizes in a quite complicated structure. This is the phase marked as $Be_{4.9}B_{13.5}$ in the experimental phase diagram (Figure 1). It has also been assumed that BeB_2 would crystallize, as does MgB_2, in the AlB_2 structure,[77–79] and this is especially true in several computational contributions following the discovery of superconductivity in MgB_2.[80–82] It is not quite as simple: we find that at atmospheric pressure, the most stable structure for BeB_2 is cubic, with a diamondoid boron network and beryllium atoms occupying interstitial tetrahedral sites.[18] This structure can be understood in terms of the Zintl–Klemm concept,[54,83] since beryllium donates its electrons to a (B^-) network that is isoelectronic to carbon. This structure is semiconducting and dynamically stable.

There are a number of other structure types in the Group 2/Group 13 binaries: the $CaAl_2$ structure (space group 227, $Fd\bar{3}m$, eight formula units per cell, prototype $MgCu_2$, the cubic C15 Laves phase);[84] the $SrAl_2$ structure (space group 74, *Imma*, four formula units per cell, prototype $CeCu_2$, a structure type with hundreds of binary and ternary representatives);[85] the $CaIn_2$ and $MgGa_2$ structure (space group 194, $P6_3/mmc$, two formula units per cell);[86,87] and another $MgGa_2$ structure (space group 55, *Pbam*, eight formula units per cell).[88]

Amongst the known structure types, we find the $CaIn_2$ structure to be the most stable in the ground state. Its boron sublattice has the hexagonal diamond structure, and beryllium atoms occupy its holes. The structure can be constructed from the AlB_2 structure type by doubling the unit cell along z and introducing buckling in the graphitic B sheets so that the B atoms form a tetrahedrally connected network (see Figure 15). It is, however, unstable at low pressures towards

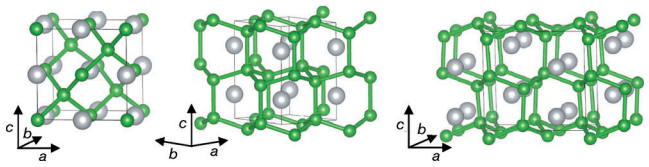

Figure 15. Ground-state BeB_2 crystal structures. From left to right: $F\bar{4}3m$, $CaIn_2$-$P6_3/mmc$, and *Pnma* structures. All at $P=1$ atm.

a symmetry-lowering that breaks the near-perfect tetrahedral B–B coordination, and moves beryllium atoms away from the centers of the cavities in the boron framework. The resulting structure, of *Pnma* symmetry, is also shown in Figure 15. The beryllium atoms are close to a buckled B_6 ring, hence shortest Be–B separations are 1.85 Å at $P=$ 1 atm, somewhat shorter than the 2.02–2.07 Å found experimentally in BeB_2C_2, which features similar coordination of Be to a six-membered mixed B/C ring.[47]

Under high pressure ($P\geq 160$ GPa), the $CaIn_2$ structure for BeB_2 is very stable and dominates the convex hull plot of the ground-state enthalpies of the Be–B phase diagram (Figure 16). From an electronegativity perspective, its stability can again be explained by beryllium donating its two valence electrons to a (B^-) network that then becomes isoelectronic to carbon, in particular hexagonal diamond. We therefore have another version of a classical Zintl system,

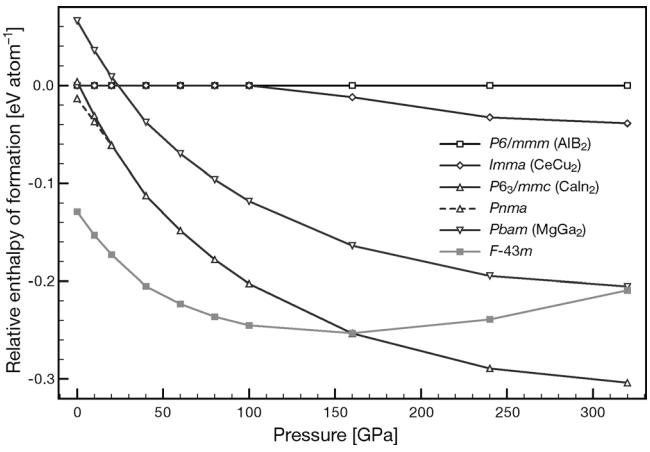

Figure 16. Ground-state enthalpies of formation of various BeB_2 phases, relative to the MgB_2 structure with *P6/mmm* symmetry. Note that the $SrAl_2$ structure transforms into the MgB_2 structure at low pressures.

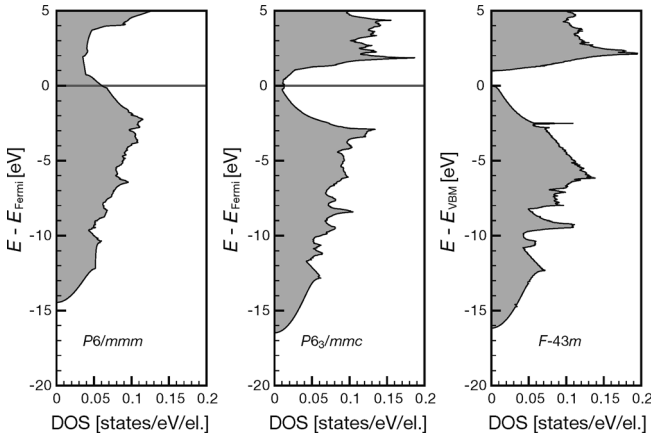

Figure 17. Electronic DOS per electron for BeB_2 in various structure types (space groups indicated), all at $P=1$ atm.

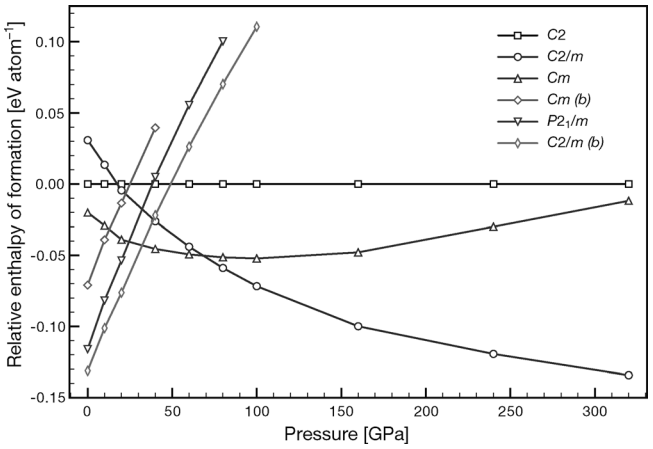

Figure 18. Ground-state enthalpies of formation for various BeB_3 structures, shown with respect to the *C*2 structure.

typified by NaTl.[54,83] In contrast to MgB_2, which forms graphitic layers, the smaller (atomic or ionic) size of beryllium allows boron to form a three-dimensional network, which is more stable. Electronically, the transition from the $F\bar{4}3m$ structure to the $CaIn_2$ $P6_3/mmc$ structure is associated with an insulator–metal transition. In fact, all other BeB_2 structures we studied, except for the $F\bar{4}3m$ structure, are metallic (see Figure 17, and see the Supporting Information for how the DOS at the Fermi level evolves as pressure is increased).

BeB_3: A somewhat more boron-rich composition than BeB_2 is BeB_3.This stoichiometry is only found in $MgIn_3$ (space group 221, $Pm\bar{3}m$, one formula unit per cell) amongst the Group 2/Group 13 binaries, and it crystallizes in the $AuCu_3$ structure type. We find that using this structure for BeB_3 does not lead to a stable structure at any pressure studied: at $P=1$ atm, $\Delta H_f = +0.86$ eV per atom with respect to separation into the elements.

As a side note, Au_3Cu is known and has the same structure type as $AuCu_3$. It is rare that a compound A_nB_m and its "stoichiometric inverse" A_mB_n crystallize in the same structure type. Here, we find the $AuCu_3$ structure to be the most stable for Be_3B, the "inverse" of BeB_3 (see the Supporting Information for details).

We performed evolutionary structure searches for BeB_3 at $P=1$ atm and $P=160$ GPa by using $Z=4$ formula units per cell, respectively. The relative enthalpies of formation of the best candidate ground-state structures are shown in Figure 18. Two distinct classes of structures emerge, stable in different pressure regimes (within the Be–B phase diagram, BeB_3 is stable at $P \geq 160$ GPa). At low pressures, different monoclinic structures of $P2_1/m$, *Cm* and *C*2/*m* symmetry, are most stable. These structures are metallic layered compounds (see Figure 19).[18]

Under pressure and in the ground state, the graphitic boron sheets are calculated to be unstable with respect to formation of three-dimensional boron networks, as seen by the rapid destabilization of these structures portrayed in

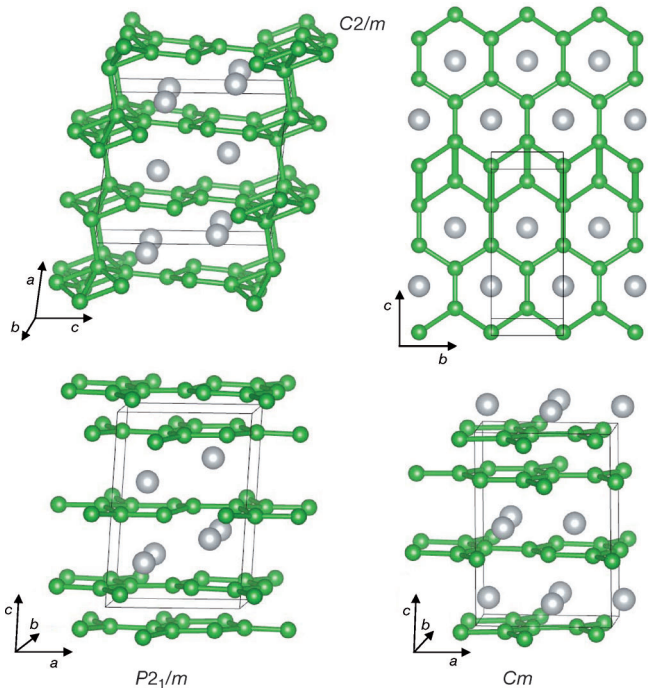

Figure 19. Predicted ground-state BeB_3 crystal structures. Top: *C*2/*m* structure, side view and top view onto B layer. Bottom left: $P2_1/m$ structure. Bottom right: *Cm* structure. All at $P=1$ atm.

Figure 18. Indeed, the high-pressure *C*2/*m* structure is similar to the $CaIn_2$ structure type, which is stable in BeB_2: we find hexagonal diamondlike boron networks with beryllium atoms in the interstitial positions. Because of the higher boron atomic content (than BeB_2), direct B–B contacts without beryllium interstitials occur (these are drawn as thick lines in Figure 20 to distinguish them from features of the $CaIn_2$ structure).

To summarize, we find very similar structural features for the high-pressure phases of BeB_2, BeB_3, and BeB_4: essentially tetrahedrally coordinated boron atoms in a lonsdaleite

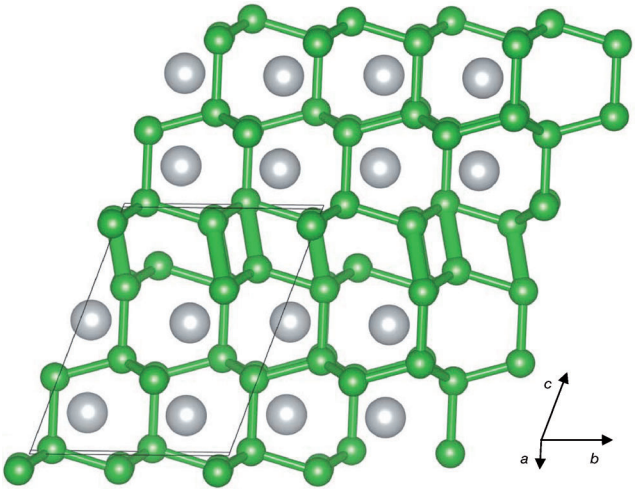

Figure 20. The ground-state high-pressure $C2/m$ structure of BeB_3, shown at $P=320$ GPa. Direct B–B separations between hexagonal diamond layers are drawn as thick lines.

arrangement, with beryllium atoms occupying interstitial sites. At high pressures, all these stoichiometries are part of the convex hull, with basically a linear dependence of the enthalpy of formation on the beryllium content. This suggests that various other stoichiometries BeB_x (with x lying between 2 and 4) could also be stable, and constructed simply by choosing the width of individual lonsdaleite-boron layers to match the respective macroscopic stoichiometry. At low pressures, the situation is different, because the phase diagram is dominated by the complex "$BeB_{2.75}$" structure, which is presented below.

"$BeB_{2.75}$": This unusual stoichiometry was assigned from analysis of single-crystal X-ray information and is associated with a large hexagonal unit cell, with (after refinement of the structure) a stoichiometry of $Be_{29.5}B_{81}$ per unit cell, which is very close to (but not quite) Be_4B_{11} or $BeB_{2.75}$.[75] The compound was found to be a superconductor.[76] The elucidation of its true structure also potentially explains discrepancies in the literature about Be–B compounds that range from BeB_2 to BeB_3.

The experimental crystal structure has partial occupancies on various lattice sites, as shown in Figure 21. We modeled this system by using the original unit cell, with stoichiometry $Be_{29}B_{81}$ (i.e, $BeB_{2.79}$, compared to $BeB_{2.75}$ in the experimental structure). In doing so, we ignored the partially occupied site Be13, which contributes another 0.5 Be atoms per unit cell when summed up over four lattice sites, each with occupancy 0.125. There are several ways to distribute the atoms over the remaining partially occupied lattice sites, and if some restrictions on minimum Be–Be and B–B separations are followed, six different unit cells (four of $P\bar{6}m2$ and two of $P3m1$ symmetry) can be constructed. The enthalpies of formation at $P=1$ atm range from $\Delta H_f=-40$–125 meV per atom for these different arrangements, thus making this compound the most stable Be–B compound in the phase diagram, and in fact the only stable binary compound up to pressures of about 20 GPa. At higher pressures, other stoichiometries are stabilized; first and foremost is BeB_2 as a Zintl compound.

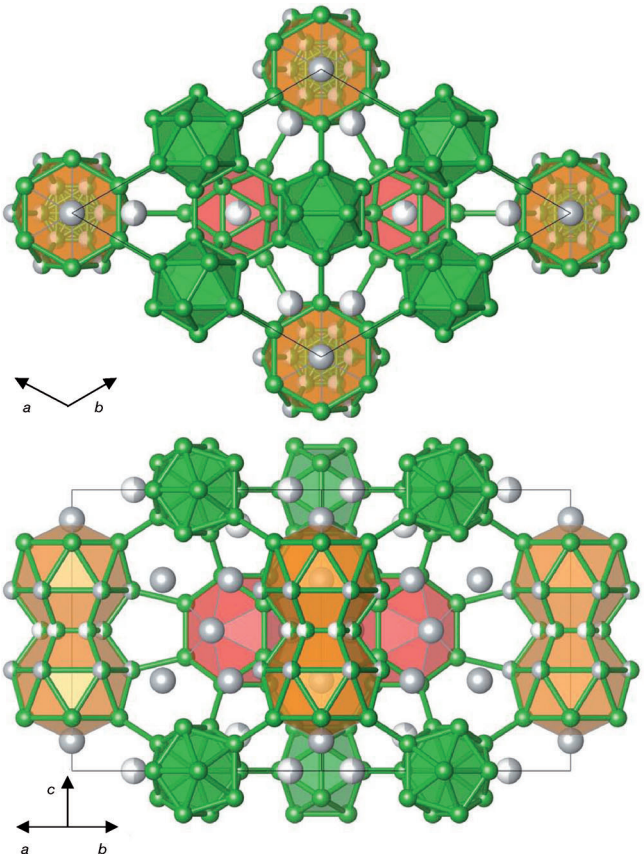

Figure 21. Experimental crystal structure of "$BeB_{2.75}$" at $P=1$ atm and $T=120$ K,[75] as seen along the c axis (top) and within the ab plane (bottom). Green (gray) spheres denote boron (beryllium) atoms, and partially filled spheres indicate partially occupied lattice sites. Green polyhedra indicate B_{12} icosahedra, red polyhedra the Be_3B_{12} units, and orange polyhedra the Be_6B_{21} units with most of the partial occupancies (see ref. [18]).

More details on the stability of $Be_{29}B_{81}$, and the manner in which its electronic properties relate to its polyhedral structural motifs, can be found in our full paper on this phase.[18] Here, our purpose is to point out that the polyhedral skeleton of the structure is complemented by beryllium atoms in various interstitial sites. This allows for the construction of structures of slightly different stoichiometries by systematically filling specific cavities in the polyhedral backbone of $BeB_{2.79}$. The relative enthalpies of formation of these different phases, as dependent on pressure, are shown in Figure 22, together with the phases BeB_2, BeB_3, and BeB_4. In fact, only one of those phases is competitive in enthalpic terms, namely, that of $Be_{26}B_{84}$ stoichiometry. This structure is semiconducting, as it conforms to the polyhedral electron-sum rules.[89,90] It is constructed by assigning half of the mixed Be/B occupied lattice sites to boron atoms alone. This phase is close to the convex hull at 1 atm, and also part

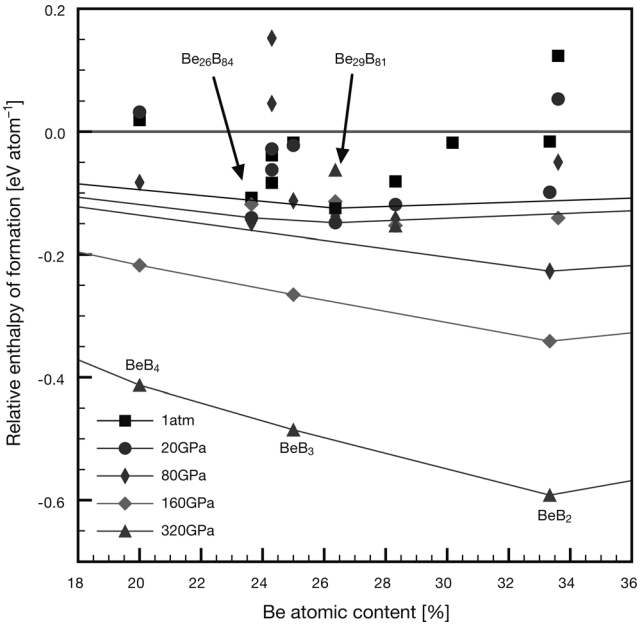

Figure 22. Ground-state enthalpies of formation per atom for $BeB_{2.75}$-based structures. The convex hulls at the various pressures are drawn.

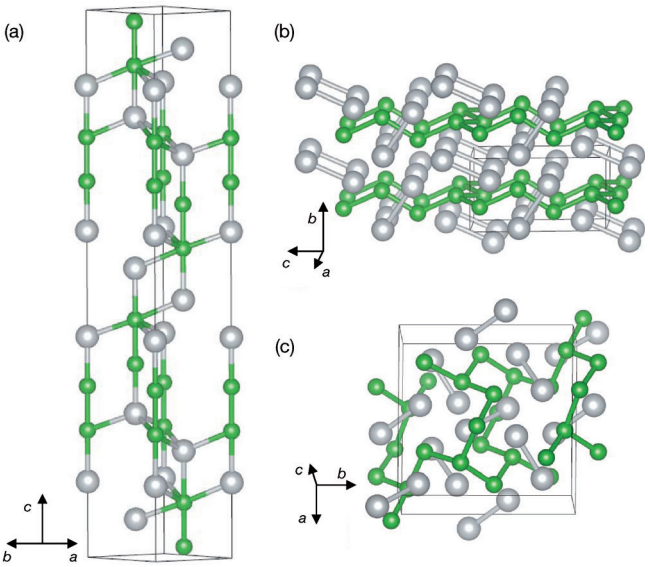

Figure 23. Enthalpically favored ground-state BeB structures at various pressures: a) hexagonal unit cell of $R\bar{3}m$ structure of BeB, at $P=1$ atm; b) the $C2/m$ structure, obtained from an evolutionary structure search, at $P=60$ GPa; and c) the $I4_1/a$ structure, found in MgGa, at $P=100$ GPa.

of it at low pressures ($P=20$ GPa). However, the BeB_2, BeB_3, and BeB_4 structures discussed earlier are far more stable at high pressures than this or any other phase subsequently derived from $BeB_{2.79}$.

The 1:1 compound BeB: Stoichiometries of 1:1 grace many phase diagrams, but to date BeB has not been found experimentally. We attempted at some length to find a suitable structure, but, as will be seen, we are only able to report that it does not come close to stability in our calculations. Among the other elements of Groups 2 and 13, this stoichiometry is found in the MgIn structure (prototype CuAu, space group $P4/mmm$, one formula unit per cell),[91] the CaIn structure (prototype CsCl, space group $Pm\bar{3}m$, one formula unit per cell),[92] the CaGa structure (prototype TlI, space group $Cmcm$, four formula units per cell),[93] and the MgGa structure (prototype LiSi, space group $I4_1/a$, 16 formula units per cell).[50] The latter is shown in Figure 23: the MgGa structure consists of two interpenetrating networks of Be dimers and B atoms. The CuAu structure found in MgIn is not enthalpically competitive in our calculations.

We also performed an evolutionary structure search at $P=60$ GPa, with four formula units per cell. From a variety of low enthalpy structural candidates, two structures emerged that are competitive at low pressures (see Figure 24). These structures, of $R\bar{3}m$ and $C2/m$ symmetry, respectively, are shown in Figure 23. The $R\bar{3}m$ structure has linear Be-B-B-Be units, but these are within bonding separations of each other, as the coordination polyhedra (in the Supporting Information) clearly show. Hence, this is a fully three-dimensional structure, with each Be atom tenfold-coordinated, and each B atom eightfold-coordinated. The $C2/m$ structure, however, consists of two-dimensional buckled B sheets that are interpenetrated and also separated by Be dimers. These dimers (Figure 23 shows the structure at $P=60$ GPa) will merge under even higher pressure to form a three-dimensional beryllium network.

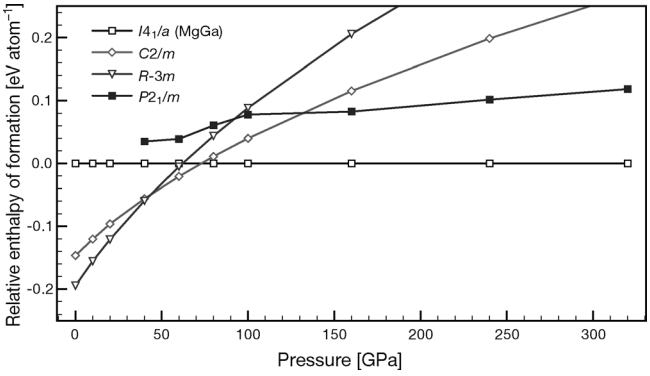

Figure 24. Relative ground-state enthalpies of various BeB crystal structures. The reference line is the high-pressure $I4_1/a$ structure.

At high pressures, $P \geq 80$ GPa, the $I4_1/a$ structure found in MgGa is enthalpically favored, as seen in Figure 24. In this structure, and in line with an ionic (Zintl) view of the structure as $Be^{2+}B^{2-}$, the five-valence-electron boron atoms should be capable of forming three bonds, and are indeed threefold-connected to other boron atoms. This feature is commonly found in the crystal structures of Group 15 elements P, As, and Sb, and the $I4_1/a$ structure is metastable: at high pressure it is a local minimum as indicated by a phonon analysis; but it is not stable, for example, at 160 GPa, with respect to decomposition into BeB_2 and Be_5B_2.

All BeB structures are metallic at all pressures; see Figure 25 below for their electronic densities of states per electron at atmospheric pressure. Note that the $R\bar{3}m$ structure features 1) a square or step onset of the DOS at low energies, indicative of a two-dimensional electron system, and 2) a pronounced pseudogap at 3 eV above the Fermi energy, which corresponds to a valence electron count of 22 electrons per unit cell (there are 20 in BeB, with $Z=4$), and thus the composition BeB_3 (with $Z=2$).

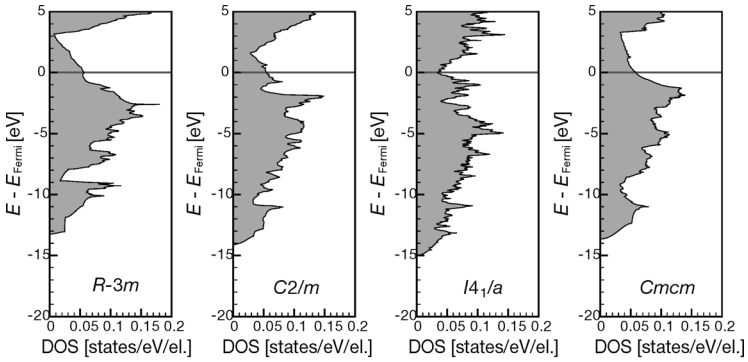

Figure 25. Electronic DOS of various ground-state BeB crystal structures (space groups indicated), all at $P=1$ atm. Note in particular that all structures are metallic.

Returning to the unusual finding of *no* range of stability for a 1:1 stoichiometry, two comments may be made on BeB:

1) The eutectic in the experimental phase diagram of Be/B (Figure 1) is not very deep. There is just a relatively small depression from the Be melting point. To the extent that a eutectic is the outcome of both entropic stabilization and electronic enthalpy preference, the "weak" eutectic is an indication to us that in liquid Be–B effective interactions are not much more effective (i.e., more stabilizing) than Be–Be, or B–B. This is consistent with no great stabilization for a 1:1 phase even in a ground state.
2) Although no BeB phase, under various pressure conditions, ever reaches the global stability line, structures of this stoichiometry are also never far away from it. In other words, there is not a compelling energetic gain for the decomposition of BeB into other stoichiometries. Although we cannot estimate reliably barriers for such transformations (and they might be very low), the lack of any large stabilization enthalpies on decomposition of BeB might make possible its synthesis as a metastable compound.

Yet other stoichiometries

Be_5B_2: We calculated this compound, stabilized under high pressures, in the orthorhombic space group 72, *Ibam*, with four formula units per cell; its prototype is the Mg_5Ga_2 structure.[50] In this structure, Be_5B_2 features single boron atoms in tenfold cavity sites of a network of beryllium atoms (see the Supporting Information). We find the ground state of this phase to be enthalpically stable under high pressures. It is again a metallic phase at all pressures; its electronic stability is recognized by the position of the Fermi energies in distinct pseudogaps.

$Be_{17}B_{12}$: This is again a quite unusual stoichiometry, but is found in $Mg_{17}Al_{12}$, the γ phase of the Mg–Al phase diagram. It crystallizes in space group $I\bar{4}3m$, in the crystal structure of α-Mn (Pearson symbol cI58).[94,95] We find the ground state for this phase to be significantly stabilized at high pressures, almost reaching the convex hull of absolute stability at $P=$ 320 GPa. This structure features beryllium atoms placed at the center of Z16 Frank–Kasper polyhedra of Be_4B_{12} composition. Bridging beryllium atoms then connect these polyhedra.

Conclusion

What is presented herein summarizes our current theoretical understanding of the ground-state region of the Be–B binary phase diagram, predicts structures for some compounds for which such structures are not yet known, and explores the evolution of stable phases with increased pressure. There are many such. The stoichiometries computed to be stable or close to stability are shown in Figure 26, a schematic diagram that gives the evolution of the stable and metastable phases with increased pressure.

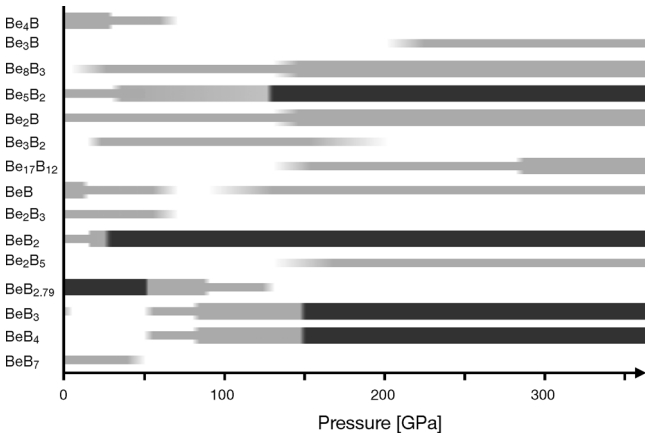

Figure 26. The stable ground-state compounds in the Be–B phase diagram, and their evolution with pressure. Wide dark grey bars indicate stable phases, wide (narrow) light grey bars indicate metastable that which are at most 50 meV per atom (100 meV per atom) removed from the global stability line.

At atmospheric pressure, we find only $BeB_{2.79}$ (a complex phase by all accounts) to be stable with respect to decomposition into the constituent elements. Several compounds are

close to stability, most prominently Be_4B. The stoichiometry Be_2B_3 is known only as a high-temperature phase; we suggest that it could be stable at lower temperatures as well. But the structure of this phase is not known experimentally; we suggest a structure of $R\bar{3}m$ symmetry with interesting linear Be-B_3-Be units for Be_2B_3. We also suggest possible structures for the compound BeB_4, a structure of $P2_12_12_1$

symmetry that is related to the MgB_4 structure type and has the lowest enthalpy at atmospheric pressure; it should quickly be replaced by any of different structures under increasing pressure, most notably a *Cmcm* structure that shares certain features with the Z phase of carbon. However, we find the BeB_4 stoichiometry to be enthalpically stable in its ground state only at high pressures. For the Be_2B phase, experimentally seen at high temperatures, but calculated here in its ground state, we find an alternative to the known fluorite structure, which is of $C2/m$ symmetry and features localized B_2 pairs surrounded by a beryllium network. We find this structure to be slightly more stable than the fluorite structure, and to be even further stabilized under pressure; an experimental study should detect here a phase transition.

In general, given the great variety of metastable structures found at every pressure, the mode of synthesis might have an effect on what stoichiometry is found experimentally. This is not an attempt to escape the responsibility of the theorist to predict; it is a statement of experimental reality. With increasing pressure, stoichiometries on the boron-richer side of the phase diagram are more stabilized. We have not included the most boron-rich compounds known in our calculations, as they feature partially occupied lattice sites and are computationally too complex for us at this time. But on the beryllium-rich side, a variety of stoichiometries are close to absolute ground-state stability under high pressures, and probably within the error bars of the calculations. These include the Be_8B_3 (see the Supporting Information), Be_5B_2, Be_2B, and $Be_{17}B_{12}$ stoichiometries and structures.

Overall, the BeB_2 phase dominates the convex hull of the ground-state regions at intermediate and high pressures, along with BeB_3, BeB_4, and Be_5B_2.The stoichiometric BeB_2 can be described as a Zintl phase, and several structure types typically found in Zintl phases are competitive in this compound. Whereas all the other structures we have found are metallic, albeit with the Fermi level falling in a pseudogap of varying depth and breadth, in the low- and intermediate-pressure range the BeB_2 phase is semiconducting. It becomes metallic at high pressures. We never find a stable ground-state 1:1 phase at any pressure, though this stoichiometry does come close to stability (and we cannot comment on the role of temperature).

Our calculations provide a range of detailed predictions of structures for known stoichiometry but unknown structure at $P=1$ atm, and of the structures, some unexpected, available to the Be–B system at elevated pressures.

Acknowledgements

Support for our work comes solely from EFree, an Energy Frontier Research Center funded by the U.S. Department of Energy (award number DESC0001057 at Cornell). Computational resources provided by the Cornell NanoScale Facility (supported by the National Science Foundation through grants ECS-0335765 and DMR-0907425), and by the XSEDE network (provided by the National Center for Supercomputer Applications through grant TG-DMR060055N), are gratefully acknowledged.

[1] W. J. Evans, M. J. Lipp, H. Cynn, C. S. Yoo, M. Somayazulu, D. Häusermann, G. Shen, V. Prakapenka, *Phys. Rev. B* **2005**, *72*, 094–113.
[2] L. X. Benedict, T. Ogitsu, A. Trave, C. J. Wu, P. A. Sterne, E. Schwegler, *Phys. Rev. B* **2009**, *79*, 064–106.
[3] N. N. Greenwood, A. Earnshaw in *Chemistry of the Elements*, Butterworth-Heinemann, Oxford, **1998**, pp. 139–215.
[4] A. R. Oganov, J. Chen, C. Gatti, Y. Ma, Y. Ma, C. W. Glass, Z. Liu, T. Yu, O. O. Kurakevych, V. L. Solozhenko, *Nature* **2009**, *457*, 863–867.
[5] E. Y. Zarechnaya, L. Dubrovinsky, N. Dubrovinskaia, Y. Filinchuk, D. Chernyshov, V. Dmitriev, N. Miyajima, A. El Goresy, H. F. Braun, S. Van Smaalen, *Phys. Rev. Lett.* **2009**, *102*, 185501.
[6] B. Albert, H. Hillebrecht, *Angew. Chem.* **2009**, *121*, 8794–8824; *Angew. Chem. Int. Ed.* **2009**, *48*, 8640–8668.
[7] G. Will, K. Ploog, *Nature* **1974**, *251*, 406–408.
[8] G. Will, B. Kiefer, *Z. Anorg. Allg. Chem.* **2001**, *627*, 2100.
[9] D. E. Sands, J. L. Hoard, *J. Am. Chem. Soc.* **1957**, *79*, 5582–5583.
[10] R. E. Hughes, C. H. L. Kennard, D. B. Sullenger, H. A. Weakliem, D. E. Sands, J. L. Hoard, *J. Am. Chem. Soc.* **1963**, *85*, 361–362.
[11] V. V. Brazhkin, T. Taniguichi, M. Akaishi, S. V. Popova, *J. Mater. Res.* **2004**, *19*, 1643–1648.
[12] R. L. Falge Jr., *Phys. Lett. A* **1967**, *24*, 579–580.
[13] M. I. Eremets, V. V. Struzhkin, H. Mao, R. J. Hemley, *Science* **2001**, *293*, 272–274.
[14] G. Federici, C. H. Skinner, J. N. Brooks, J. P. Coad, C. Grisolia, A. A. Haasz, A. Hassanein, V. Philipps, C. S. Pitcher, J. Roth, *Nucl. Fusion* **2001**, *41*, 1967–2137.
[15] M. Wang, Y. Li, T. Cui, Y. Ma, G. Zou, *Appl. Phys. Lett.* **2008**, *93*, 101905.
[16] H. Okamoto, L. E. Tanner in *Binary Alloy Phase Diagrams* (Eds.: T. B. Massalski, H. Okamoto, P. R. Subramanian, L. Kacprzak), ASM International, Materials Park, **1990**, p. 460.
[17] P. Villars, H. Okamoto, K. Cenzual, *ASM Alloy Phase Diagrams Center*, ASM International, Materials Park, **2006**.
[18] A. Hermann, N. W. Ashcroft, R. Hoffmann, *Inorg. Chem.* **2012**, *51*, 9066–9075.
[19] F. X. Zhang, F. F. Xu, T. Tanaka, *J. Solid State Chem.* **2004**, *177*, 3070–3074.
[20] G. Kresse, J. Furthmüller, *Phys. Rev. B* **1996**, *54*, 11169–11186.
[21] P. E. Blöchl, *Phys. Rev. B* **1994**, *50*, 17953–17979.
[22] G. Kresse, D. Joubert, *Phys. Rev. B* **1999**, *59*, 1758–1775.
[23] J. P. Perdew, K. Burke, M. Ernzerhof, *Phys. Rev. Lett.* **1996**, *77*, 3865–3868.
[24] D. Alfè, *Comput. Phys. Commun.* **2009**, *180*, 2622–2633.
[25] D. C. Lonie, E. Zurek, *Comput. Phys. Commun.* **2011**, *182*, 372.
[26] D. C. Lonie, E. Zurek, *Comput. Phys. Commun.* **2012**, *183*, 690–697.
[27] K. Momma, F. Izumi, *J. Appl. Crystallogr.* **2011**, *44*, 1272–1276.
[28] H. Rosner, W. E. Pickett, *Phys. Rev. B* **2003**, *67*, 054104.
[29] M. Wörle, R. Nesper, T. K. Chatterji, *Z. Anorg. Allg. Chem.* **2006**, *632*, 1737–1742.
[30] K. Schubert, K. Frank, R. Gohle, A. Maldonado, H. G. Meissner, A. Raman, W. Rossteutscher, *Naturwissenschaften* **1963**, *50*, 41a.
[31] B. Huang, J. D. Corbett, *Inorg. Chem.* **1998**, *37*, 5827–5833.
[32] G. S. Smith, Q. Johnson, D. N. Wood, *Acta Crystallogr. Sect. B* **1969**, *25*, 554–557.
[33] D. E. Sands, C. F. Cline, A. Zalkin, C. L. Hoenig, *Acta Crystallogr.* **1961**, *14*, 309–310.

[34] A. Belsky, M. Hellenbrandt, V. L. Karen, P. Luksch, *Acta Crystallogr. Sect. B* **2002**, *58*, 364–369.
[35] G. Bergerhoff, I. D. Brown in *Crystallographic Databases* (Eds.: F. H. Allen, G. Bergerhoff, R. Sievers), Chester: International Union Of Crystallography, **1987**, pp. 77–95.
[36] B. Hartke, *J. Phys. Chem.* **1993**, *97*, 9973–9976.
[37] R. L. Johnston, *Dalton Trans.* **2003**, 4193.
[38] B. Assadollahzadeh, P. R. Bunker, P. Schwerdtfeger, *Chem. Phys. Lett.* **2008**, *451*, 262–269.
[39] A. R. Oganov, A. O. Lyakhov, M. Valle, *Acc. Chem. Res.* **2011**, *44*, 227–237.
[40] N. N. Greenwood, A. Earnshaw in *Chemistry of the Elements*, Butterworth-Heinemann, Oxford, **1998**, pp. 107–138.
[41] D. F. Gaines, K. M. Coleson, J. C. Calabrese, *J. Am. Chem. Soc.* **1979**, *101*, 3979–3980.
[42] A. B. Burg, H. I. Schlesinger, *J. Am. Chem. Soc.* **1940**, *62*, 3425–3429.
[43] J. F. Stanton, W. N. Lipscomb, R. J. Bartlett, *J. Chem. Phys.* **1988**, *88*, 5726–5734.
[44] D. S. Marynick, W. N. Lipscomb, *Inorg. Chem.* **1972**, *11*, 820–823.
[45] J. C. Calabrese, D. F. Gaines, S. J. Hildebrandt, J. H. Morris, *J. Am. Chem. Soc.* **1976**, *98*, 5489–5492.
[46] R. J. Gilliard, M. Y. Abraham, Y. Wang, P. Wei, Y. Xie, B. Quillian, H. F. Schaefer, P. V. R. Schleyer, G. H. Robinson, *J. Am. Chem. Soc.* **2012**, *134*, 9953–9955.
[47] K. Hofmann, X. Rocquefelte, J.-F. Halet, C. Bähtz, B. Albert, *Angew. Chem.* **2008**, *120*, 2333–2336; *Angew. Chem. Int. Ed.* **2008**, *47*, 2301–2303.
[48] H. J. Becher, A. Schäfer, *Z. Anorg. Allg. Chem.* **1962**, *318*, 304–312.
[49] G. Gundersen, L. Hedberg, K. Hedberg, *J. Chem. Phys.* **1973**, *59*, 3777.
[50] K. Schubert, F. Gauzzi, K. Frank, *Z. Metallk.* **1963**, *54*, 422.
[51] K. Frank, K. Schubert, *J. Less-Common Met.* **1970**, *20*, 215.
[52] W. Müller, *Z. Naturforsch. B* **1977**, *32*, 357–359.
[53] G. A. Papoian, R. Hoffmann, *Angew. Chem.* **2000**, *112*, 2500–2544; *Angew. Chem. Int. Ed.* **2000**, *39*, 2408–2448.
[54] E. Zintl, W. Dullenkopf, *Z. Phys. Chem. Abt. B* **1932**, *16*, 195–205.
[55] W. Klemm, *Proc. Chem. Soc.* **1958**, 329.
[56] *Chemistry, Structure, and Bonding of Zintl Phases and Ions* (Ed.: S. M. Kauzlarich), Wiley-VCH, New York, Weinheim, **1996**.
[57] Z. Liu, X. Qu, B. Huang, Z. Li, *J. Alloys Compd.* **2000**, *311*, 256–264.
[58] A. Hermann, A. Suarez-Alcubilla, I. G. Gurtubay, L.-M. Yang, A. Bergara, N. W. Ashcroft, R. Hoffmann, *Phys. Rev. B* **2012**, *86*, 144110.
[59] I. R. Shein, A. L. Ivanovskii, *Phys. Status Solidi B* **2001**, *227*, R1–R3.
[60] J. Moussa, J. Noffsinger, M. Cohen, *Phys. Rev. B* **2008**, *78*, 104506.
[61] H. L. Luo, C. C. Chao, P. Duwez, *Trans. Metall. Soc. AIME* **1964**, *230*, 1488–1490.
[62] Y. Feutelais, B. Legendre, N. Rodier, V. Agafonov, *Mater. Res. Bull.* **1993**, *28*, 591–596.
[63] A. D. Becke, K. E. Edgecombe, *J. Chem. Phys.* **1990**, *92*, 5397.
[64] M. M. Roger Naslain, A. Guette, M. Barret, *J. Solid State Chem.* **1973**, *8*, 68–85.
[65] R. Schmitt, B. Blaschkowski, K. Eichele, H.-J. Meyer, *Inorg. Chem.* **2006**, *45*, 3067–3073.
[66] Z. Liu, X. Han, D. Yu, Y. Sun, B. Xu, X.-F. Zhou, J. He, H.-T. Wang, Y. Tian, *Appl. Phys. Lett.* **2010**, *96*, 031903.
[67] M. Ben Yahia, O. Reckeweg, R. Gautier, J. Bauer, T. Schleid, J.-F. Halet, J.-Y. Saillard, *Inorg. Chem.* **2008**, *47*, 6137–6143.
[68] G. Bruzzone, *Acta Crystallogr.* **1965**, *18*, 1081–1082.
[69] G. Bruzzone, M. L. Fornasini, F. Merlo, *J. Less-Common Met.* **1989**, *154*, 67–77.
[70] S. Andersson, J.-O. Carlsson, E. E. Astrup, S. Liaaen-Jensen, A. Lamvik, E. Sunde, N. A. Sørensen, *Acta Chem. Scand.* **1970**, *24*, 1791–1799.
[71] A. Knappschneider, C. Litterscheid, J. Kurzman, R. Seshadri, B. Albert, *Inorg. Chem.* **2011**, *50*, 10540–10542.
[72] M. Amsler, J. Flores-Livas, L. Lehtovaara, F. Balima, S. Ghasemi, D. Machon, S. Pailhès, A. Willand, D. Caliste, S. Botti, *Phys. Rev. Lett.* **2012**, *108*, 065501.
[73] L. Y. Markovskii, Y. A. Kondrashev, G. V. Kaputovskaia, *Zhur. Obshch. Khim. USSR* **1955**, *25*, 1045.
[74] R. Mattes, K.-F. Tebbe, H. Neidhard, H. Rethfeld, *J. Less-Common Met.* **1976**, *47*, 29–32.
[75] J. Y. Chan, F. R. Fronczek, D. P. Young, J. F. DiTusa, P. W. Adams, *J. Solid State Chem.* **2002**, *163*, 385–389.
[76] D. Young, R. Goodrich, P. Adams, J. Chan, F. Fronczek, F. Drymiotis, L. Henry, *Phys. Rev. B* **2002**, *65*, 180518.
[77] M. S. Borovikova, V. V. Fesenko, *J. Less-Common Met.* **1986**, *117*, 287–291.
[78] J. E. Hirsch, *Phys. Lett. A* **2001**, *282*, 392–398.
[79] I. Felner, *Physica B+C* **2001**, *353*, 11–13.
[80] J. Nagamatsu, N. Nakagawa, T. Muranaka, Y. Zenitani, J. Akimitsu, *Nature* **2001**, *410*, 63–64.
[81] P. Singh, *Phys. Rev. Lett.* **2001**, *87*, 87004.
[82] N. Medvedeva, A. Ivanovskii, J. Medvedeva, A. Freeman, *Phys. Rev. B* **2001**, *64*, 020502.
[83] H. Schäfer, B. Eisenmann, W. Müller, *Angew. Chem.* **1973**, *85*, 742–760; *Angew. Chem. Int. Ed. Engl.* **1973**, *12*, 694–712.
[84] T. Rivillo, W. E. Wallace, *J. Solid State Chem.* **1980**, *31-35*, 309.
[85] G. Cordier, E. Czech, H. Schäfer, *Z. Naturforsch. B* **1982**, *37*, 1442.
[86] A. Iandelli, *Z. Anorg. Allg. Chem.* **1964**, *330*, 221–232.
[87] G. Nuspl, K. Polborn, J. Evers, G. A. Landrum, R. Hoffmann, *Inorg. Chem.* **1996**, *35*, 6922–6932.
[88] G. S. Smith, K. F. Mucker, Q. Johnson, D. H. Wood, *Acta Crystallogr. Sect. B* **1969**, *25*, 549–553.
[89] K. Wade, *J. Chem. Soc. D* **1971**, 792.
[90] M. Tillard-Charbonnel, A. Manteghetti, C. Belin, *Inorg. Chem.* **2000**, *39*, 1684–1696.
[91] N. Ino, M. Hirabayashi, S. Ogawa, *Trans. Jap. Inst. Metals* **1965**, *6*, 172–178.
[92] G. Bruzzone, A. F. Ruggiero, *J. Less-Common Met.* **1964**, *7*, 368–372.
[93] W. Harms, M. Wendorff, C. Röhr, *J. Alloys Compd.* **2009**, *469*, 89–101.
[94] J.-C. Crivello, T. Nobuki, T. Kuji, *Intermetallics* **2007**, *15*, 1432–1437.
[95] N. Wang, W.-Y. Yu, B.-Y. Tang, L.-M. Peng, W.-J. Ding, *J. Phys. D* **2008**, *41*, 195408.

Received: October 30, 2012
Published online: February 11, 2013

